



# Modelling the effect of UV light at different wavelengths and treatment combinations on the inactivation of *Campylobacter jejuni*

Arturo B. Soro<sup>a,c</sup>, Paul Whyte<sup>c</sup>, Declan J. Bolton<sup>b</sup>, Brijesh K. Tiwari<sup>a,\*</sup>

<sup>a</sup> Department of Food Chemistry and Technology, Teagasc Food Research Centre, Ashtown, Dublin 15, Ireland

<sup>b</sup> Department of Food Safety, Teagasc Food Research Centre, Ashtown, Dublin 15, Ireland

<sup>c</sup> UCD School of Veterinary Medicine, University College Dublin, Belfield, Dublin 4, Ireland

## ARTICLE INFO

### Keywords:

Modelling

UV light

Light-emitting diodes (LED)

*Campylobacter jejuni*

Survival curves

Combination of wavelengths

## ABSTRACT

Application of novel decontamination strategies such as Ultraviolet (UV) irradiation are required to mitigate the risks associated with *Campylobacter jejuni* in food. This study evaluated the use of a light-emitting diode (LED) based technology to inactivate *C. jejuni* NCTC 11168 in Maximum Recovery Diluent (MRD) at wavelengths of 280, 300 and 365 nm and combinations. To assess the survival curves, two linear (Log linear (LL) and Linear and Shoulder) and two non-linear models (Weibull and Double Weibull) were fitted. UV exposures showed different antimicrobial effects where a combination of 280/300 nm was the most effective treatment with a  $4D_1$  value of 5 s observed in a bacterial suspension of 5 log CFU/mL. Moreover, the LL model was the most robust model to describe the inactivation kinetics of *Campylobacter* when exposed to UV and therefore, modelling tools could be applied to predict the efficiency of UV light in a model solution.

Industrial relevance: Light-based technologies like UV light are identified in the literature as potential alternatives to assure the decontamination of surfaces, liquids and solid food. However, some of these techniques require further investigation. The present study evaluated the use of a LED system and effect of combined wavelengths in the inactivation of *Campylobacter* through predictive modelling. This technique was observed to predict and explain kinetics of inactivation of *Campylobacter* and could be key in the scaling-up process of UV light at industrial level.

## 1. Introduction

In the last several decades, campylobacteriosis has been reported as the most prevalent bacterial zoonotic disease in Europe. In 2017, cases of campylobacteriosis represented 70% of all cases of foodborne diseases within European countries (EFSA & ECDC, 2018). *Campylobacter jejuni* is associated with 84% of all reported cases in Europe (EFSA & ECDC, 2017). This foodborne pathogen is a spiral-shaped Gram-negative bacterium that belongs to the Campylobacteraceae family. Moreover, mammals and birds are frequently colonised by *C. jejuni* which can grow optimally under low oxygen concentrations at temperatures between 37 and 42 °C (Silva et al., 2011). Principal vehicles of *Campylobacter* infection are associated with the handling or consumption of undercooked broiler meat and raw milk and contaminated ready-to-eat food products as a result of the cross-contamination with raw products (Johnson, Shank, & Johnson, 2017). Factors such as high initial concentrations in the gastrointestinal tracts of animals, cross-contamination along the

food chain, resistance of cells to food processing, among others, have contributed to the high prevalence of *Campylobacter* at retail level (Sarp, Hanninen, & Rautelin, 2016). Thus, current measures are focused on the prevention of *Campylobacter* contamination and reduction of its prevalence in foods. However, ongoing efforts by health protection agencies and producers should be directed to ensure the correct application of current measures and to identify new procedures or technologies (Vinueza-Burgos, Cevallos, Cisneros, Van Damme, & De Zutter, 2018).

Ultraviolet (UV) irradiation is situated in the wavelength range of 100 and 400 nm of the light spectrum. Some authors divide the UV spectrum in three different portions: UV-C (200–280 nm), UV-B (280–315 nm) and UV-A (315–400 nm) where UV-C has demonstrated the highest bactericidal effects (Delorme et al., 2020). In recent years, UV light technology has evolved and is now available as highly efficient and low cost devices known as UV light-emitting diodes (LED) which use semiconducting materials to emit radiation (Song, Mohseni, &

\* Corresponding author.

E-mail addresses: [paul.whyte@ucd.ie](mailto:paul.whyte@ucd.ie) (P. Whyte), [declan.bolton@teagasc.ie](mailto:declan.bolton@teagasc.ie) (D.J. Bolton), [brijesh.tiwari@teagasc.ie](mailto:brijesh.tiwari@teagasc.ie) (B.K. Tiwari).

<https://doi.org/10.1016/j.ifsset.2021.102626>

Received 29 October 2020; Received in revised form 13 January 2021; Accepted 21 January 2021

Available online 27 January 2021

1466-8564/© 2021 Published by Elsevier Ltd.

Taghipour, 2016). Koutchma and Popović (2019) highlighted the ability of these devices to use combined UV light wavelengths and concluded that the synergistic effect of these UV treatments could be applied to inactive foodborne pathogens in the food industry. For instance, Song, Mohseni, and Taghipour (2019) observed that the combination of 265 and 365 nm wavelengths decreased the reactivation of *Escherichia coli* in water. Further investigation is required to assess the synergistic effects of multiple wavelengths against common foodborne pathogens. Soro, Whyte, Bolton, and Tiwari (2020) reviewed the efficacy of UV light to decrease the concentration of *Campylobacter* in poultry meat and highlighted its promising results. However, additional work is required to assess the effects of applying combinations of different wavelength treatments on bacterial pathogens.

Mathematical models are descriptive and predictive tools which can be developed to help our understanding of microbial and quality changes that may occur during food processing. Moreover, modelling techniques are based on previous experimental data and model parameters can depend on many factors such as temperature, time or bacterial species. In particular, microbial models (growth or inactivation) study the biological variability of microorganisms and can aid risk assessment approaches (Garre, Zwietering, & den Besten, 2020). To the best of our knowledge the present study is the first to apply a modelling approach to investigate the effect of different UV wavelengths and combinations on *Campylobacter*. In the literature, other authors have investigated the use of mathematical models to assess the effect of UV light on other bacterial species such as *E. coli*, *Listeria innocua*, *Bacillus subtilis*, *Alicyclobacillus acidoterrestris*, *Pseudomonas aeruginosa*, *Legionella pneumophila* or *Salmonella Typhimurium* in water, liquids and solid food (Baysal, Molva, & Unluturk, 2013; Gayan, Manas, Alvarez, & Condon, 2013; Gayán, Monfort, Álvarez, & Condón, 2011; Hinds, Charoux, Akhter, O'Donnell, & Tiwari, 2020; Mutz, Rosario, Bernardes, Paschoalin, & Conte-Junior, 2020; Quintero-Ramos, Churey, Hartman, Barnard, & Worobo, 2004; Rattanukul & Oguma, 2018; Unluturk, Atilgan, Baysal, & Unluturk, 2010; Zhou, Li, Lan, Yan, & Zhu, 2017). Such data is also required to evaluate the inactivation of *Campylobacter* cells through exposure to UV irradiation. Moreover, the combination of multiple wavelength should be evaluated as a potential strategy to increase the efficiency of UV treatments to inhibit this foodborne pathogen.

The aim of the present study was to compare the efficiency of UV light wavelengths of 280, 300 and 365 nm and combinations of 280 + 300, 280 + 365 and 280 + 300 + 365 nm to inactivate *C. jejuni* NCTC 11168 in MRD. This study applied a modelling technique to evaluate and predict the inactivation effect of a UV-LED based technology through the estimation of D values in four survival linear and non-linear models.

## 2. Materials and methods

### 2.1. Bacterial culture preparation

*Campylobacter jejuni* NCTC 11168 was selected from the microbiology stock cultures at Teagasc Food Research Centre Ashtown (Dublin, Ireland) to carry out this study. The bacterial culture was preserved at  $-80^{\circ}\text{C}$  on protective beads in defibrinated horse blood (Oxoid, UK). *Campylobacter* stock was placed onto Mueller Hinton agar plates (Oxoid, UK) for bacterial resuscitation and incubated inside a sealed jar at  $42^{\circ}\text{C}$  for 48 h under a microaerobic atmosphere of 5%  $\text{O}_2$ , 15%  $\text{CO}_2$ , and 85%  $\text{N}_2$  using Campygen 2.5 (Oxoid, UK) and 3.5 L (Oxoid, UK) sachets. Isolated colonies were streaked onto modified charcoal cefoperazone deoxycholate agar (mCCDA, Oxoid, UK) supplemented with *Campylobacter* growth supplement (Oxoid, UK) and incubated microaerobically for 48 h at  $42^{\circ}\text{C}$ . To avoid bacterial damage, singles colonies were obtained from fresh cultures every 2–3 days to conduct the study.

### 2.2. LED equipment

The LED equipment (PearlLab Beam, Aquisense technologies, NC,

**Table 1**

Measurements of the intensity/fluence rate of UV light for each applied wavelength at different time points.

Wavelength (nm)	Treatment times (s)	Intensity/fluence rate ( $\text{W}/\text{cm}^2$ )
280	2, 3, 4, 5, 6, 7, 8	0.068
300	2, 10, 14, 18, 22, 26, 28	0.049
365	30, 45, 60, 90, 120, 135, 150	0.043
280 + 300	1, 2, 3, 4, 5, 6, 7	0.112
280 + 365	2, 3, 4, 5, 6, 7, 8	0.106
280 + 300 + 365	2, 3, 4, 5, 6, 7, 8	0.146

USA) comprised of cylindrical chamber, LED lamp and control box. Samples were placed into the UV chamber and treated with the selected wavelengths of  $280 \pm 1$ ,  $300 \pm 4$  and  $365 \pm 3$  nm with a full bandwidth of 12.4, 16.9 and 8.9 nm at half of the maximum, respectively, and combinations at different time points as Table 1 shows. UV light intensity or fluence rate was measured with a radiometer (Opticalmeter, model ILT2400, International light technologies, MA, USA) in the centre of the machine (Table 1).

### 2.3. Inactivation experiments with UV light

Isolated colonies on mCCDA plates were aseptically inoculated in 30 mL of Mueller Hinton Broth (CM0405, Oxoid) and incubated for 48 h at  $42^{\circ}\text{C}$  in microaerobic conditions. After incubation, cell suspensions were centrifuged at 7500 xg for 10 min and twice washed with 30 mL of maximum recovery diluent (MRD, Oxoid), a transparent solution that contributes to the osmotic balance of bacteria. Serial dilutions in MRD were performed to obtain a *C. jejuni* concentration of  $\sim 5$  log CFU/mL in a final suspension of 10 mL. Concentration of the inoculum was confirmed to avoid a protective effect against UV light due to high bacterial content and ensure accurate inactivation kinetics of the cells. The 10-mL volume bacterial suspensions were poured into glass petri dishes (without lid) with a liquid depth of  $\sim 6$  mm and volume capacity of  $24 \text{ cm}^3$  (Height: 1.3 cm and Diameter: 5.8 cm); and centrally placed into the LED chamber at a distance from the source of 5 cm. To assay the effectiveness of the UV light, the individual and combination treatments were performed using several time points (Table 1). Untreated samples with the inoculated bacteria were considered as controls following same procedure. UV treatments were assessed in duplicate and three independent experiments were carried out.

### 2.4. Microbiological analysis

After UV exposure, *Campylobacter* concentrations were determined

**Table 2**

Equations of the models fitted for the inactivation curves of *C. jejuni* NCTC 11168 after the application of UV light.

Model	Equation
Log Linear (LL)	$\log_{10}(N) = \log_{10}(N_0) - \frac{K_{\max} \times t}{\ln(10)}$
Log Linear and Shoulder (LS)	$\log_{10}(N) = \log_{10}(N_0) - \frac{K_{\max} \times t}{\ln(10)} + \log_{10}\left(\frac{e^{K_{\max} \times SL}}{(1 + (e^{K_{\max} \times SL} - 1) \times e^{K_{\max} \times t})^p}\right)$
Weibull (W)	$\log_{10}(N) = \log_{10}(N_0) - \left(\frac{t}{\delta_1}\right)^p$
Double Weibull (DW)	$\log_{10}(N) = \log_{10}\left[\left(\frac{10^{N_0}}{1 + 10^\alpha}\right) \times 10^{-\left(\frac{t}{\delta_1}\right)^p + \alpha}\right] + 10^{-\left(\frac{t}{\delta_2}\right)^p}$

N is the bacterial concentration;  $N_0$  is the initial bacterial concentration;  $K_{\max}$  is the first order constant of inactivation; t is the treatment time; SL is the parameter of shoulder length; p is a shape parameter;  $\delta_1$  and  $\delta_2$  are scale parameters and  $\alpha$  is a physiological parameter linked with  $\delta_1$ .

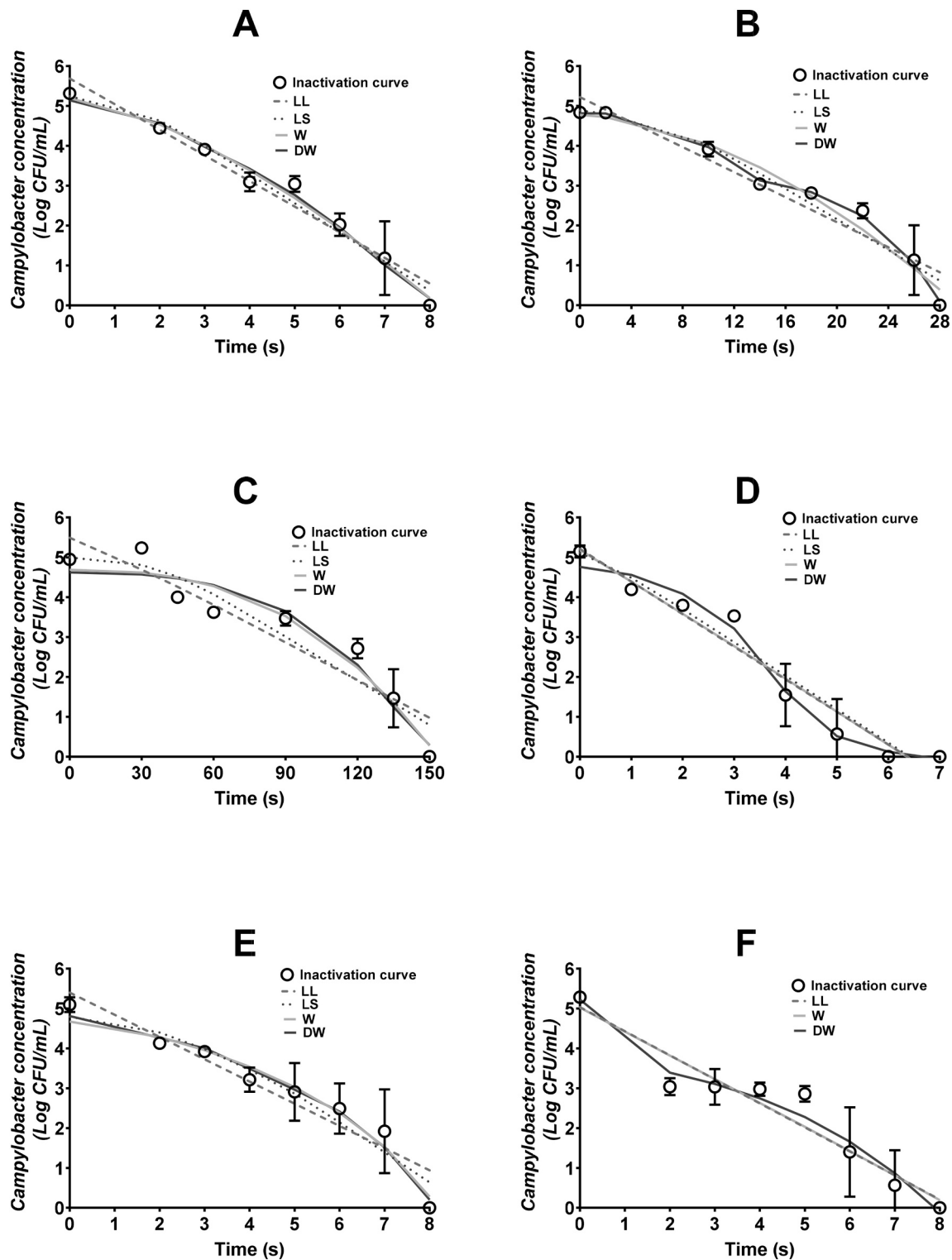


Fig. 1. Inactivation curves of *C. jejuni* NCTC 11168 with UV light at wavelengths of 280 (A), 300 (B), 365 (C), 280 + 300 (D), 280 + 365 (E) and 280 + 300 + 365 (F) nm and fitted with models: Log Linear (LL), Log linear and Shoulder (LS), Weibull (W) and Double Weibull (DW).

in the bacterial suspensions of treated and control samples. Serial 10-fold dilutions in MRD were prepared and a 0.1-mL aliquots were plated onto mCCDA plates. The mCCDA plates were incubated for 48 h at 42 °C in microaerobic conditions. After incubation bacterial colonies were enumerated and the mean counts of treatments and controls were calculated. Finally, bacterial concentrations were expressed in CFU log units per mL of MRD treated.

### 2.5. Inactivation models

Different models were assessed to fit the inactivation curves of *C. jejuni* NCTC 11168 obtained after UV light exposure experiments. The Microsoft® excel component of GInaFIT was employed in the analysis of the microbial data and selection of the most suitable models to fit the inactivation of *Campylobacter* (Geeraerd, Valdramidis, & Van Impe,

**Table 3**Calculated parameters of the models for the destruction of *C. jejuni* NCTC 11168 with UV light at different wavelengths (nm).

Model	Parameter	Treatment (nm)					
		280	300	365	280 + 300	280 + 365	280 + 300 + 365
LL	Kmax	1.48 ± 0.13 <sup>a</sup>	0.36 ± 0.03 <sup>b</sup>	0.07 ± 0.00 <sup>c</sup>	1.88 ± 0.10 <sup>d</sup>	1.28 ± 0.14 <sup>e</sup>	1.39 ± 0.12 <sup>ae</sup>
LS	Kmax	1.69 ± 0.24 <sup>f</sup>	0.46 ± 0.05 <sup>g</sup>	0.09 ± 0.00 <sup>g</sup>	1.94 ± 0.07 <sup>f</sup>	1.74 ± 0.60 <sup>f</sup>	–
	SL	1.28 ± 0.53 <sup>h</sup>	6.55 ± 1.09 <sup>i</sup>	36.14 ± 4.14 <sup>j</sup>	0.34 ± 0.27 <sup>h</sup>	2.11 ± 1.50 <sup>h</sup>	–
W	δ	2.66 ± 0.32 <sup>k</sup>	11.94 ± 0.84 <sup>l</sup>	85.17 ± 8.26 <sup>m</sup>	1.29 ± 0.34 <sup>k</sup>	3.96 ± 1.68 <sup>k</sup>	1.71 ± 0.56 <sup>k</sup>
	p	1.47 ± 0.19 <sup>n</sup>	1.74 ± 0.20 <sup>n</sup>	2.65 ± 0.34 <sup>n</sup>	1.03 ± 0.13 <sup>n</sup>	2.94 ± 2.71 <sup>n</sup>	1.04 ± 0.25 <sup>n</sup>
DW	α	2.79 ± 1.85 <sup>op</sup>	2.22 ± 1.28 <sup>p</sup>	4.88 ± 0.18 <sup>o</sup>	4.62 ± 0.36 <sup>o</sup>	2.16 ± 1.62 <sup>p</sup>	3.05 ± 1.70 <sup>op</sup>
	δ <sub>1</sub>	2.72 ± 0.68 <sup>q</sup>	10.55 ± 1.28 <sup>r</sup>	90.22 ± 10.16 <sup>s</sup>	2.38 ± 0.45 <sup>q</sup>	2.63 ± 1.62 <sup>q</sup>	1.01 ± 0.45 <sup>q</sup>
	δ <sub>2</sub>	49,390.98 ± 83,967.61 <sup>t</sup>	21.32 ± 4.19 <sup>t</sup>	1062.06 ± 2388.11 <sup>t</sup>	365,645.05 ± 808,989.04 <sup>t</sup>	2996.90 ± 7326.17 <sup>t</sup>	7,017,219.93 ± 17,188,597.20 <sup>t</sup>
	p	2.59 ± 0.79 <sup>u</sup>	5.05 ± 1.63 <sup>u</sup>	3.26 ± 1.38 <sup>u</sup>	2.57 ± 1.63 <sup>u</sup>	4.55 ± 1.88 <sup>u</sup>	2.57 ± 1.37 <sup>u</sup>

Results calculated as Mean ± Standard Deviation where significant differences do not share the same superscript letter ( $p < 0.05$ ).

Abbreviations: LL (Log Linear), LS (Log linear and Shoulder), W (Weibull), DW (Double Weibull).

Parameters in blank space did not fit the inactivation curve.

2005). The four selected models were two linear: Log Linear (LL) and Log Linear and Shoulder (LS); and non-linear: Weibull (W) and Double Weibull (DW) with associated equations presented in Table 2. Moreover, constants of these inactivation models were calculated for every UV light treatment. Log linear models assumed that bacterial cells have similar resistance to the effect of a disinfection technology (Cole, Davies, Munro, Holyoak, & Kilsby, 1993). However, it was demonstrated that some groups of cells can develop resistance at the beginning of the treatment and therefore, the Log linear and shoulder model was postulated (Geeraerd, Herremans, & Van Impe, 2000). Furthermore, the curve models of Weibull and Double Weibull described the inactivation of bacterial cells as more irregular and complex systems dependent on shape and size parameters (Mafart, Couvert, Gaillard, & Leguerinel, 2002).

To select the most appropriate model or models, the time to achieve a 4 log CFU/mL reduction in the bacterial population ( $4D_t$ ) and parameters of goodness of the fit such as the regression coefficient ( $R^2$ ), root mean square error (RMSE), Akaike's Information Criterion (AIC) and Bayesian's Information Criterion (BIC) were considered. Thus,  $4D_t$ ,  $R^2$  (eq. 1) and RMSE (eq. 2) values were obtained with the GnaFIT tool (Geeraerd, Herremans, & Van Impe, 2005). In addition, the quality of fitting capacity of the models was determined by calculating AIC (eq. 3) and BIC (eq. 4) for all the UV treatments (Zhu, Zhang, Hinds, Sun, & Tiwari, 2020).

$$R^2 = \frac{\sum (C_p - C_o)^2}{N - n} \quad (1)$$

$$RMSE = \sqrt{\frac{\sum (C_p - C_o)^2}{N - n}} \quad (2)$$

$$AIC = N \ln\left(\frac{SE}{N}\right) + 2(n+1) + \frac{2(n+1)(n+2)}{N - n - 2} \quad (3)$$

$$BIC = N \ln\left(\frac{SE}{N}\right) + (n+1) + \ln(n) \quad (4)$$

Where  $C_p$  and  $C_o$  represent the predictive and observed concentration of bacteria, SE is the sum of the square error, N is the number of observations and n is the number of parameters in the studied model.

## 2.6. Statistical analysis

Treatments with UV light were developed per duplicate in three independent experiments ( $n = 6$ ) and the obtained inactivation curves were fitted in the former models. The average and standard deviation of the parameters for the fitted models and  $4D_t$  values were statistically evaluated and detected using factorial analysis of variance (ANOVA) combined with the Tukey *post hoc* test at a significance level of  $p < 0.05$ . The statistical programs employed were GraphPad Prism 7 and

Minitab® 17.

## 3. Results and discussion

The inactivation curves of *C. jejuni* NCTC 11168 (Fig. 1) were fitted into the survival models of LL, LS, W and DW (Table 2) to describe the antimicrobial effect of the UV light wavelengths of 280 (Fig. 1 A), 300 (Fig. 1 B) and 365 (Fig. 1 C) nm and combinations of 280 + 300 (Fig. 1 D), 280 + 365 (Fig. 1 E) and 280 + 300 + 365 nm (Fig. 1 F). The total concentration of *Campylobacter* was plotted against the treatment time until complete inactivation was determined. In general, there was a clear difference in the effectiveness of UV light between wavelengths and their combinations. Treatment times to achieve total bacterial inactivation were of 8, 28, 150, 7, 8 and 8 s for wavelengths of 280, 300, 365, 280 + 300, 280 + 365 and 280 + 365 + 365 nm, respectively. In particular, the combination of the 365 nm wavelength with 280 nm strongly reduced the time by approximately 140 s for total inactivation of *C. jejuni* cells. Authors like Koutchma and Popović (2019) and Hinds et al. (2020) also observed the synergic effect of applying multiple wavelength combinations for the inactivation of bacterial cells and therefore, could contribute to increased efficacy of UV treatments.

Parameters of the survival models are presented in Table 3 and significant differences ( $p < 0.05$ ) were detected in levels of bacterial reduction between the different UV treatments. Linear models are simply characterised by the constant of inactivation or  $K_{max}$  which is the inverse of the  $D_t$ . Hence,  $K_{max}$  values closer to one result in higher inactivation rates. Additionally, these systems can be complemented with a shoulder length factor or SL to describe the protective effect against cell damage in the first stages. In this way, survival models with higher SL values were initially more resistant to the effect of UV light than others (Geeraerd, Herremans, & Van Impe, 2005). Fitted LL and LS models for the inactivation curves of 300 and 365 nm presented the lowest  $K_{max}$  and highest SL compared to the other UV treatments ( $p < 0.05$ ) (Table 3). Moreover, values of SL in the 280 nm model were not significantly different ( $p \geq 0.05$ ) from the models for the combined wavelength treatments resulting in lower resistance rates to the effect of UV light. A similar pattern in the inactivation rate values or  $\delta$  and  $\delta_1$  was observed in W and DW models, respectively. These scale parameters had lower values for the inactivation curves of 280 nm and the combination of 300 and 365 nm treatments ( $p < 0.05$ ) showing an increased bactericidal effect. In addition, scale parameters of the models were dependent on the shape constant of p with values greater than one resulting in convex curves. Scanlon et al. (2015) observed comparable results in the shape parameters of the Weibull models and associated bacterial resistance against the thermal effect with p values higher than one. All of the inactivation curves fitted with W and DW followed the same trend and no significant differences were detected ( $p \geq 0.05$ ). Moreover, the DW model describes the different behaviour of two sub-populations of bacterial cells: sensitive ( $\delta_1$ ) and resistant ( $\delta_2$ ) groups to the antimicrobial



**Table 4**

4D values and goodness parameters calculated for each model and treatment with UV light to inactivate *C. jejuni* NCTC 11168.

Treatment (nm)	Model	4 D <sub>t</sub> value (s)	Goodness of model			
			R <sup>2</sup>	RMSE	AIC	BIC
280	LL	6.32 ± 0.55	(0.90–0.95)	0.49 ± 0.08	-7.57 ± 2.64	-13.97 ± 2.64
		6.87 ± 0.31	(0.90–0.96)	0.46 ± 0.07	-4.30 ± 2.33	-14.22 ± 2.33
	6.93 ± 0.32	(0.91–0.96)	0.42 ± 0.06	-5.89 ± 2.36	-15.81 ± 2.36	
	DW	6.95 ± 0.35	(0.92–0.97)	0.40 ± 0.07	19.53 ± 2.80	-13.53 ± 2.80
300	LL	25.81 ± 1.71	(0.87–0.92)	0.57 ± 0.07	-4.94 ± 1.78	-11.34 ± 1.78
		28.81 ± 1.03	(0.89–0.93)	0.53 ± 0.04	-1.97 ± 1.32	-11.89 ± 1.32
	26.81 ± 0.93	(0.90–0.93)	0.48 ± 0.02	-3.66 ± 0.70	-13.58 ± 0.70	
	DW	26.60 ± 0.66	(0.91–0.98)	0.34 ± 0.11	16.55 ± 4.87	-16.52 ± 4.87
365	LL	132.50 ± 8.98*	(0.82–0.86)	0.73 ± 0.06	-0.97 ± 1.30	-7.37 ± 1.30
		145.00 ± 5.90	(0.82–0.88)	0.71 ± 0.06	2.75 ± 1.23	-7.17 ± 1.23
	145.00 ± 4.90	(0.86–0.91)	0.60 ± 0.05	0.12 ± 1.38	-9.80 ± 1.38	
	DW	144.80 ± 5.43	(0.83–0.88)	0.67 ± 0.04	27.91 ± 1.01	-5.15 ± 1.01
280 + 300	LL	4.95 ± 0.24	(0.82–0.96)	0.61 ± 0.18	-4.63 ± 4.70	-11.03 ± 4.70
		5.12 ± 0.39	(0.90–0.95)	0.60 ± 0.12	-0.87 ± 3.60	-10.79 ± 3.58
	4.96 ± 0.49	(0.79–0.95)	0.65 ± 0.20	0.62 ± 5.01	-9.30 ± 5.01	
	DW	4.75 ± 0.59	(0.95–0.98)	0.41 ± 0.04	-8.00 ± 1.70	-17.92 ± 1.70
280 + 365	LL	7.16 ± 0.59	(0.66–0.91)	0.67 ± 0.13	-2.71 ± 3.25	-9.11 ± 3.25
		7.55 ± 0.38	(0.61–0.94)	0.66 ± 0.16	1.16 ± 4.24	-8.76 ± 4.24
	7.54 ± 0.41	(0.79–0.96)	0.58 ± 0.13	-1.13 ± 4.45	-11.05 ± 4.45	
	DW	7.60 ± 0.32	(0.84–0.99)	0.49 ± 0.17	21.64 ± 7.11	-11.43 ± 7.11
280 + 300 + 365	LL	6.72 ± 0.58	(0.69–0.87)	0.73 ± 0.12	-1.24 ± 2.55	-7.64 ± 2.55
		6.68 ± 0.54	(0.66–0.86)	0.78 ± 0.12	4.11 ± 2.44	-5.81 ± 2.44
	DW	6.56 ± 0.43	(0.57–0.97)	0.68 ± 0.28	26.64 ± 7.35	-6.43 ± 7.35

Results calculated as Mean ± Standard Deviation.

Abbreviations: Log Linear (LL), Log linear and Shoulder (LS), Weibull (W), Double Weibull (DW), regression coefficient (R<sup>2</sup>), root mean square error (RMSE), Akaike's Information Criterion (AIC), Bayesian's Information Criterion (BIC).

Significant differences of \*p < 0.05 were obtained after comparison between inactivation models of the same treatment.

effect of a technological process. The DW equation consists of two coupled Weibull models in order to express the differences in resistance between cells. At the same time, DW models incorporate the new parameter of  $\alpha$  which is the logit of the  $\delta_1$  fraction in the total bacterial population and linked to their physiological state (Coroller, Leguerinel, Mettler, Savy, & Mafart, 2006). In general, the values for the subpopulation of resistant bacteria ( $\delta_2$ ) tended towards the infinite for all the UV treatments and significant differences ( $p < 0.05$ ) were found in the values of the sensitive group of cells ( $\delta_1$ ) for the 300 and 365 nm treatments compared to the other UV exposures (Table 3). In other words, there was a decrease in levels of the sensitive group of bacteria of the former treatments resulting in a higher proportion of cells resistant to the effect of UV.

Goodness of fit parameters and 4D<sub>t</sub> values are shown in Table 4. Four decimal reductions or 4D<sub>t</sub> of *C. jejuni* concentrations were reached at time points ranked from 4.75 to 145.00 s among all the UV treatments in which the lowest and highest 4D<sub>t</sub> values are from samples treated with 280 + 300 and 365 nm, respectively. Furthermore, 4D<sub>t</sub> values of the models were not statistically different except for a reduction of 12 s in the 4D<sub>t</sub> of the survival curve of 365 nm fitted with the LL model ( $p < 0.05$ ). In concordance with Fig. 1, the wavelength combination of 280 and 300 nm had demonstrated a reduction in *Campylobacter* levels of 4 log CFU/mL at 4.75–5.12 s treatments and thus, were the most effective UV treatments for the inactivation of this pathogen in a liquid model. Other authors have also investigated the effect of UV light on *Campylobacter* strains. For instance, Murdoch, Maclean, MacGregor, and Anderson (2010) observed a reduction of 5 log CFU/mL after the application of 405-nm light for 30 min in a liquid solution with *C. jejuni* LMG 8841. In another study, UV light at 254 nm was applied during 8 s in a 7-log bacterial solution of *C. jejuni* NCTC 11168 and a reduction of 5 log CFU/mL was observed (Haughton et al., 2011). Moreover, the efficacy of UV light of the former and present study was similar the same strain of *Campylobacter* is compared. Haughton et al. (2012) studied the effect of UV light at 395 nm in a liquid suspension of *C. jejuni* NCTC 11168 and observed a reduction of 5 log CFU/mL following a 30-s treatment. Although previous studies have confirmed the antimicrobial effect of UV light on *Campylobacter*, to the best of our knowledge, the present study is the first that uses modelling to predict the impact of this technology using multiple wavelengths and combinations.

The goodness of the fit of the models was analysed through the parameters of R<sup>2</sup>, RMSE, AIC and BIC (Table 4). According to Inguglia, Tiwari, Kerry, and Burgess (2018), models with R<sup>2</sup> values closer to one are considered to have a higher performance of fit. Additionally, parameters of RMSE, AIC and BIC with low values also indicate good fit performance and are required in combination with R<sup>2</sup> in order to successfully compare between models. In general, the goodness of the fit varied in all the models. The LL model was shown to have the best goodness of fit compared to all the selected models where R<sup>2</sup>, RMSE, AIC and BIC values ranked from 0.66–0.96, 0.49–0.73, -(0.97–7.57) and -(7.37–13.97), respectively. The difference between real and predictive values was also plotted (Supplementary materials). Although all of the models had good correlations between the real and model values (R<sup>2</sup> > 0.85), the Double Weibull model showed the best correlation (R<sup>2</sup>: 0.90–0.98) ( $p < 0.001$ ) in all of the survival curves (Fig. S.4). Furthermore, there was a clear difference on the goodness of fit parameters between UV exposures. In particular, models fitted in the survival curve of 280 nm had better goodness parameters than those fitted in the curves of 280 + 300, 280 + 365 and 280 + 300 + 365 nm (Table 4). Therefore,

the application of UV light alone or in combination with other wavelengths may have contributed to the goodness of the fit. There is not enough evidence in the literature that supports the use of modelling to predict the effect of UV light for the inactivation of *Campylobacter*. Chun, Kim, Chung, Won, and Song (2009) investigated the inactivation kinetics of *C. jejuni* ATCC 19111 with a linear and Weibull model in a ready-to-eat pork-based product after exposure to UV light at 254 nm. These authors observed that high intensities of UV light did not reduce the concentration of the bacteria, and thus, linear and Weibull models were not a good fit for *Campylobacter* inactivation.

#### 4. Conclusion

The present study observed dissimilarities in the effectiveness of different UV wavelengths and combinations for the decontamination of *C. jejuni* NCTC 11168 in liquid. In particular, the combination of 280 and 300 nm was the most effective treatment with a  $4D_t$  value of approximately 5 s. Moreover, the survival models showed different performance in the goodness of fit. The models for the combined wavelengths had a lower goodness of fit with the survival curves. Overall, the LL model was the most robust model which may adequately describe the inactivation kinetics of *Campylobacter*. Thus, this study demonstrated how modelling tools can be used to predict and evaluate the efficacy of UV light as a decontamination technology. Finally, future research should focus on the evaluation of the effect of combined UV wavelengths and use of predictive models for food safety purposes.

#### Declaration of Competing Interest

None.

#### Acknowledgments

This study was financed by Teagasc Walsh Fellowship program, Department of Agriculture, Food, and Marine (DAFM) under the Food Institutional Research Measure (FIRM) program [Grant number: DAFM/17/F/275].

#### Appendix A. Supplementary data

Supplementary data to this article can be found online at <https://doi.org/10.1016/j.ifset.2021.102626>.

#### References

- Baysal, A. H., Molva, C., & Unluturk, S. (2013). UV-C light inactivation and modeling kinetics of *Alicyclobacillus acidoterrestris* spores in white grape and apple juices. *International Journal of Food Microbiology*, 166(3), 494–498. <https://doi.org/10.1016/j.ijfoodmicro.2013.08.015>
- Chun, H., Kim, J., Chung, K., Won, M., & Song, K. B. (2009). Inactivation kinetics of *Listeria monocytogenes*, *Salmonella enterica* serovar Typhimurium, and *Campylobacter jejuni* in ready-to-eat sliced ham using UV-C irradiation. *Meat Science*, 83(4), 599–603. <https://doi.org/10.1016/j.meatsci.2009.07.007>
- Cole, M. B., Davies, K. W., Munro, G., Holyoak, C. D., & Kilsby, D. C. (1993). A vitalistic model to describe the thermal inactivation of *Listeria monocytogenes*. *Journal of Industrial Microbiology*, 12(3), 232–239. <https://doi.org/10.1007/BF01584195>
- Coroller, L., Leguerinel, I., Mettler, E., Savy, N., & Mafart, P. (2006). General model, based on two mixed weibull distributions of bacterial resistance, for describing various shapes of inactivation curves. *Applied and Environmental Microbiology*, 72(10), 6493–6502. <https://doi.org/10.1128/AEM.00876-06>
- Delorme, M. M., Guimarães, J. T., Coutinho, N. M., Balthazar, C. F., Rocha, R. S., Silva, R., ... Cruz, A. G. (2020). Ultraviolet radiation: An interesting technology to preserve quality and safety of milk and dairy foods. *Trends in Food Science & Technology*, 102, 146–154. <https://doi.org/10.1016/j.tifs.2020.06.001>
- EFSA & ECDC. (2017). The European Union summary report on trends and sources of zoonoses, zoonotic agents and food-borne outbreaks in 2016. *EFSA Journal*, 15(12), Article e05077. <https://doi.org/10.2903/j.efsa.2017.5077>
- European Food Safety Authority (EFSA) and European Centre for Disease Prevention and Control (ECDC). (2018). The European Union summary report on trends and sources of zoonoses, zoonotic agents and food-borne outbreaks in 2017. *EFSA Journal*, 16(12). <https://doi.org/10.2903/j.efsa.2018.5500>
- Garre, A., Zwietering, M. H., & den Besten, H. M. W. (2020). Multilevel modelling as a tool to include variability and uncertainty in quantitative microbiology and risk assessment. Thermal inactivation of *Listeria monocytogenes* as proof of concept. *Food Research International*, 137. <https://doi.org/10.1016/j.foodres.2020.109374>
- Gayán, E., Manas, P., Alvarez, I., & Condon, S. (2013). Mechanism of the synergistic inactivation of *Escherichia coli* by UV-C light at mild temperatures. *Applied and Environmental Microbiology*, 79(14), 4465–4473. <https://doi.org/10.1128/AEM.00623-13>
- Gayán, E., Monfort, S., Álvarez, I., & Condon, S. (2011). UV-C inactivation of *Escherichia coli* at different temperatures. *Innovative Food Science & Emerging Technologies*, 12(4), 531–541. <https://doi.org/10.1016/j.ifset.2011.07.008>
- Geeraerd, A. H., Herremans, C. H., & Van Impe, J. F. (2000). Structural model requirements to describe microbial inactivation during a mild heat treatment. *International Journal of Food Microbiology*, 59(3), 185–209. [https://doi.org/10.1016/S0168-1605\(00\)00362-7](https://doi.org/10.1016/S0168-1605(00)00362-7)
- Geeraerd, A. H., Valdramidis, V. P., & Van Impe, J. F. (2005). GlnaFIT, a freeware tool to assess non-log-linear microbial survivor curves. *International Journal of Food Microbiology*, 102(1), 95–105. <https://doi.org/10.1016/j.ijfoodmicro.2004.11.038>
- Haughton, P. N., Grau, E. G., Lyng, J., Cronin, D., Fanning, S., & Whyte, P. (2012). Susceptibility of *Campylobacter* to high intensity near ultraviolet/visible 395+/-5nm light and its effectiveness for the decontamination of raw chicken and contact surfaces. *International Journal of Food Microbiology*, 159(3), 267–273. <https://doi.org/10.1016/j.ijfoodmicro.2012.09.006>
- Haughton, P. N., Lyng, J. G., Cronin, D. A., Morgan, D. J., Fanning, S., & Whyte, P. (2011). Efficacy of UV light treatment for the microbiological decontamination of chicken, associated packaging, and contact surfaces. *Journal of Food Protection*, 74(4), 565–572. <https://doi.org/10.4315/0362-028X.JFP-10-356>
- Hinds, L. M., Charoux, C. M. G., Akhter, M., O'Donnell, C. P., & Tiwari, B. K. (2020). Effectiveness of a novel UV light emitting diode based technology for the microbial inactivation of *Bacillus subtilis* in model food systems. *Food Control*, 114. <https://doi.org/10.1016/j.foodcont.2019.106910>
- Inguglia, E. S., Tiwari, B. K., Kerry, J. P., & Burgess, C. M. (2018). Effects of high intensity ultrasound on the inactivation profiles of *Escherichia coli* K12 and *Listeria innocua* with salt and salt replacers. *Ultrasonics Sonochemistry*, 48, 492–498. <https://doi.org/10.1016/j.ulsonch.2018.05.007>
- Johnson, T. J., Shank, J. M., & Johnson, J. G. (2017). Current and potential treatments for reducing *Campylobacter* colonization in animal hosts and disease in humans. *Frontiers in Microbiology*, 8, 487. <https://doi.org/10.3389/fmicb.2017.00487>
- Koutchma, T., & Popović, V. (2019). UV light-emitting diodes (LEDs) and food safety. In *Ultraviolet LED Technology for Food Applications* (pp. 91–117). <https://doi.org/10.1016/B978-0-12-817794-5.00005-4>
- Mafart, P., Couvert, O., Gaillard, S., & Leguerinel, I. (2002). On calculating sterility in thermal preservation methods: Application of the Weibull frequency distribution model. *International Journal of Food Microbiology*, 72(1), 107–113. [https://doi.org/10.1016/S0168-1605\(01\)00624-9](https://doi.org/10.1016/S0168-1605(01)00624-9)
- Murdoch, L. E., Maclean, M., MacGregor, S. J., & Anderson, J. G. (2010). Inactivation of *Campylobacter jejuni* by exposure to high-intensity 405-nm visible light. *Foodborne Pathogens and Disease*, 7(10), 1211–1216. <https://doi.org/10.1089/fpd.2010.0561>
- Mutz, Y. S., Rosario, D. K. A., Bernardes, P. C., Paschoalin, V. M. F., & Conte-Junior, C. A. (2020). Modeling *Salmonella* Typhimurium inactivation in dry-fermented sausages: Previous habituation in the food matrix undermines UV-C decontamination efficacy. *Frontiers in Microbiology*, 11, 591. <https://doi.org/10.3389/fmicb.2020.00591>
- Quintero-Ramos, A., Churey, J. J., Hartman, P., Barnard, J., & Worob, R. W. (2004). Modeling of *Escherichia coli* inactivation by UV irradiation at different pH values in apple cider. *Journal of Food Protection*, 67(6), 1153–1156. <https://doi.org/10.4315/0362-028X-67.6.1153>
- Rattanukul, S., & Oguma, K. (2018). Inactivation kinetics and efficiencies of UV-LEDs against *Pseudomonas aeruginosa*, *Legionella pneumophila*, and surrogate microorganisms. *Water Research*, 130, 31–37. <https://doi.org/10.1016/j.watres.2017.11.047>
- Scanlon, K. A., Tiwari, U., Cagney, C., Walsh, D., McDowell, D. A., & Duffy, G. (2015). Modelling the thermal inactivation of five *Campylobacteraceae* species. *Food Control*, 47, 135–140. <https://doi.org/10.1016/j.foodcont.2014.06.042>
- Silva, J., Leite, D., Fernandes, M., Mena, C., Gibbs, P. A., & Teixeira, P. (2011). *Campylobacter* spp. as a foodborne pathogen: a review. *Frontiers in Microbiology*, 2, 200. <https://doi.org/10.3389/fmicb.2011.00200>
- Skarp, C. P. A., Hanninen, M. L., & Rautelin, H. I. K. (2016). *Campylobacteriosis*: The role of poultry meat. *Clinical Microbiology and Infection*, 22(2), 103–109. <https://doi.org/10.1016/j.cmi.2015.11.019>
- Song, K., Mohseni, M., & Taghipour, F. (2016). Application of ultraviolet light-emitting diodes (UV-LEDs) for water disinfection: A review. *Water Research*, 94, 341–349. <https://doi.org/10.1016/j.watres.2016.03.003>
- Song, K., Mohseni, M., & Taghipour, F. (2019). Mechanisms investigation on bacterial inactivation through combinations of UV wavelengths. *Water Research*, 163, 114875. <https://doi.org/10.1016/j.watres.2019.114875>
- Soro, A. B., Whyte, P., Bolton, D. J., & Tiwari, B. K. (2020). Strategies and novel technologies to control *Campylobacter* in the poultry chain: A review. *Comprehensive Reviews in Food Science and Food Safety*, 19(4), 1353–1377. <https://doi.org/10.1111/1541-4337.12544>
- Unluturk, S., Atilgan, M. R., Baysal, A. H., & Unluturk, M. S. (2010). Modeling inactivation kinetics of liquid egg white exposed to UV-C irradiation. *International Journal of Food Microbiology*, 142(3), 341–347. <https://doi.org/10.1016/j.ijfoodmicro.2010.07.013>
- Vinueza-Burgos, C., Cevallos, M., Cisneros, M., Van Damme, I., & De Zutter, L. (2018). Quantification of the *Campylobacter* contamination on broiler carcasses during the slaughter of *Campylobacter* positive flocks in semi-industrialized slaughterhouses.

- International Journal of Food Microbiology*, 269, 75–79. <https://doi.org/10.1016/j.ijfoodmicro.2018.01.021>
- Zhou, X., Li, Z., Lan, J., Yan, Y., & Zhu, N. (2017). Kinetics of inactivation and photoreactivation of *Escherichia coli* using ultrasound-enhanced UV-C light-emitting diodes disinfection. *Ultrasonics Sonochemistry*, 35(Pt A), 471–477. <https://doi.org/10.1016/j.ultsonch.2016.10.028>
- Zhu, X., Zhang, Z., Hinds, L. M., Sun, D. W., & Tiwari, B. K. (2020). Applications of ultrasound to enhance fluidized bed drying of *Ascophyllum Nodosum*: Drying kinetics and product quality assessment. *Ultrasonics Sonochemistry*, 70, 105298. <https://doi.org/10.1016/j.ultsonch.2020.105298>